Journal of Colloid and Interface Science 449 (2015) 21–30

Contents lists available at ScienceDirect

Journal of Colloid and Interface Science

www.elsevier.com/locate/jcis

Poly(vinylamine) microgel–dextran composite hydrogels: Characterisation; properties and pH-triggered degradation

Judith McCann [a], Jonathan M. Behrendt [a], Junfeng Yan [a], Silvia Halacheva [b], Brian R. Saunders [a,*]

[a] Biomaterials Research Group, Manchester Materials Science Centre, School of Materials, The University of Manchester, Grosvenor Street, Manchester M1 7HS, UK
[b] University of Bolton, Institute for Materials Research and Innovation, Deane Road, Bolton, Greater Manchester BL3 5AB, UK

ARTICLE INFO

Article history:
Received 26 June 2014
Accepted 17 September 2014
Available online 28 September 2014

Keywords:
Microgel
N-vinylformamide
Polyvinylamine
Dextran
Mixed dispersion
Gel
Imine

ABSTRACT

The present study involves an investigation of the formation, characterisation and triggered-degradation of mixed dispersions involving cationic poly(vinylamine-*co*-bis(ethyl vinylamine) ether) (PVAM-BEVAME) microgel (MG) particles and partially oxidised dextran (Dexox). In this approach to colloidal hydrogel composite formation, imine bonds were formed by reaction between aldehyde groups of Dexox and the primary amine groups on the MG particles. The composite hydrogels contained MG particles that were externally cross-linked by Dexox to form an elastically effective network with high storage modulus (G') values and low $\tan\delta$ ($=G''/G'$, where G'' is the loss modulus) values. The G' values for the MG–Dexox gels increased exponentially with increasing mass ratio (*MR*) of Dexox to MG. Interestingly, the yield strains determined from rheology also increased with *MR* and yield strains of up to 130% were measured. Au nanoparticles of comparable size to the Dexox chains adsorbed to the surface of the MG particles, which suggests that the pore size of the MG particles may have been smaller than that of the Dexox coils. The MG–Dexox gels were also subjected to acidic conditions to demonstrate pH-triggered gel network breakdown via imine bond cleavage. We show that new PVAM MG/aldehyde mixtures studied here for the first time form ductile and versatile colloidal gels and our new method provides a route to increasing ductility of hydrogels containing MG particles.

1. Introduction

Microgels [1–4] (MGs) and other responsive biomaterials [5,6] continue to attract much attention in the literature. MGs are cross-linked polymer particles that swell when the pH approaches the polymer particle pK_a or when the particles are dispersed in a good solvent [7]. They have been used very effectively to prepare hydrogels, including hydrogel–MG composites and doubly crosslinked MGs [8,9] as well as tough MG-reinforced hydrogels [10]. Mixed dispersions where one or both of the components are MGs that have stimulus responsive properties have been reported [9,11]. In this study, we have investigated gels prepared from a combination of pH-responsive MG particles and partially oxidised dextran (Dexox) for the first time. Dextran (Dex) is a biocompatible, natural polymer [12] and has been widely studied in the form of Dexox due to the high concentration of synthetically useful aldehyde groups in the latter [13–16]. Maia et al. used Dexox to form injectable and degradable hydrogels [13] and have also extensively investigated the periodate oxidation reaction of Dex [17]. Here, we investigate composite hydrogels prepared by reaction of amine-rich MG particles with Dexox.

The MG used in this study, poly(vinylamine-*co*-bis(ethyl vinylamine)ether) (PVAM-BEVAME), was first reported by our group in 2013 [4]. PVAM has many functionalization options afforded by its primary amino groups and a range of potential applications [4]. PVAM-BEVAME MGs have high amine contents and are pH-responsive. In an aqueous environment, a decrease in pH causes the MGs to swell and become increasingly positively charged [4]. The present study takes advantage of an imine bond formation between the primary amine groups within the PVAM MGs and the aldehydes on Dexox (see Scheme 1). Imination has widely been studied for use in biomaterials [18] because it efficiently produces a stable, covalent linkage that can be reversibly cleaved at low pH. Here, inter-MG imine bond creation was used to trigger gel formation. Unlike previous studies which focussed on surface active properties [19], the present study involves the first report of combining Dexox and PVAM to form hydrogels to the best of our knowledge.

* Corresponding author at: Biomaterials Research Group, School of Materials, Grosvenor Street, Manchester M13 9PL, UK. Fax: +44 161 306 3586.
E-mail addresses: judith.mccann@postgrad.manchester.ac.uk (J. McCann), jonathan.behrendt@manchester.ac.uk (J.M. Behrendt), junfeng.yan@manchester.ac.uk (J. Yan), s.halacheva@bolton.ac.uk (S. Halacheva), brian.saunders@manchester.ac.uk (B.R. Saunders).

http://dx.doi.org/10.1016/j.jcis.2014.09.041
0021-9797/

Our previous studies involving covalently inter-linked MG particles [20] have revealed brittleness for hydrogels composed only of PVAM MGs. The key motivation for the present work was to test the hypothesis that replacement of some of the MG particles with flexible Dexox chains would produce a ductile network. Furthermore, the introduction of acid-cleavable imine groups was expected to introduce a means for reversing gel formation via acidification. Both of these hypotheses are explored in the present study.

The use of acid-triggered cleavage of a network based on (oxidised) dextran used here contrasts to that of Widenbring et al. [21] who demonstrated enzymatic degradation of dextran-based microgels using dextranase. Our acid-based (non-enzymatic) gel breakdown approach could have advantages for in vivo applications involving ischemic tissue environments, which are known to have intrinsically low pH values [22]. Ischemic heart disease [23] is a major health problem and would benefit from triggered release using an injectable gel. An acid-triggered cleavage mechanism may provide a faster response compared to an enzymatic cleavage approach because of the greater permeability of protons compared to enzymes within most networks.

PVAM MGs are of great interest due to their high amine proportion and versatility, which can provide for functionalization [24–26]. MGs containing PVAM have been widely studied [1,27–30]. Pelton et al. [28] prepared MGs which contain a minor proportion of PVAM and were mostly poly(*N*-isopropylacrylamide) (NIPAm). As the main approach to PVAM synthesis was via *N*-vinyl formamide with a harsh, alkaline, hydrolysis step the MGs were limited to 39 mol.% conversion. Thaiboonrod et al. [30] developed MGs which contained mostly PVAM and used a crosslinker developed by Berkland et al. [31]. The crosslinker was 2-(*N*-vinylformamido) ethyl ether (NVEE) and was not cleaved upon alkaline hydrolysis, but was hydrolysed to BEVAME. We used PVAM-BEVAME MGs in the present study as a source of primary amine groups for formation of injectable, covalently linked hydrogels (Scheme 1).

MGs that have been prepared with imine bonds as crosslinks within particles have also attracted attention recently [32–36]. Wang et al. used imine formation between aldehyde groups in Dexox and primary amine groups in poly(allyl amine) to form MG particles [34,35]. Jia et al. [36] used a similar aldehyde/amine reaction to form MG particles which were then doubly cross-linked to form a hydrogel network. Sivakumaran and Maitland [15] studied a MG-embedded hydrogel containing Dexox as the hydrogel matrix and NIPAm-based MGs. By using the latter combination they were able to tune the drug release profile of their hydrogel.

The composite depicted in Scheme 1 can be considered as a hydrogel containing embedded MG particles. In contrast to other hydrogels containing MGs [37–40], the composites studied here use the MG particles as the only network forming crosslinker. If the MG particles were to be removed then the gel would revert to the fluid state because there would not be a source of crosslinking between the Dexox chains.

The new approach used in this study was to crosslink the MG particles with Dexox to give a network which was designed to provide elasticity (via the MG component) and ductility (via the Dexox component). Non-oxidised (aldehyde-free) Dex was used as a control in order to highlight the utility of covalent imine groups in the gelation process. The novelty of this study is the formation of self-

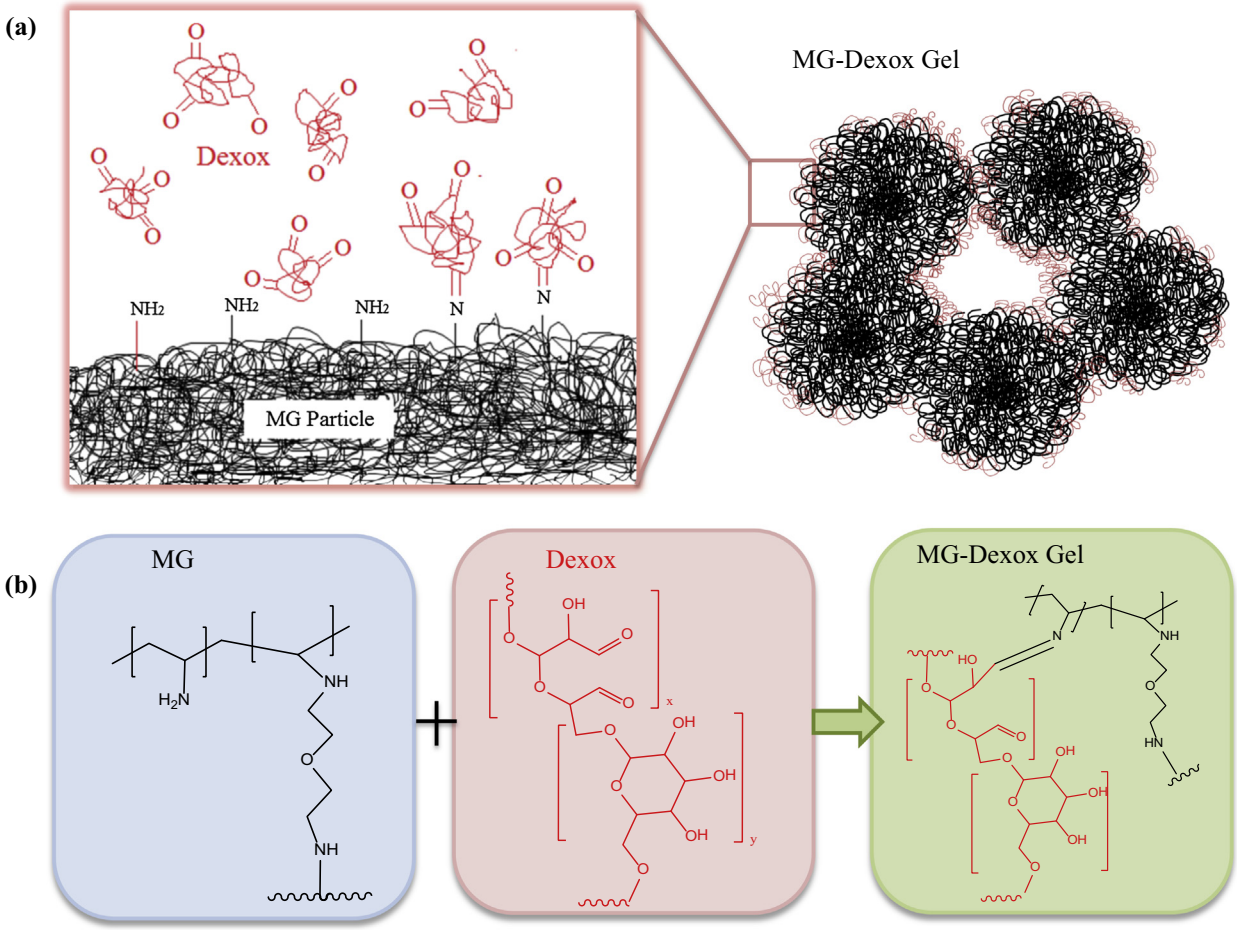

Scheme 1. Depiction of preparation of MG–Dexox composite hydrogels. (a) Gel formation and (b) the proposed reaction scheme. The MG particles and Dexox for (a) are not drawn to scale to enhance clarity.

assembled composite hydrogels using Dexox and MG particles. These gels were studied as a function of the proportions of each component and demonstrated good mechanical property tunability. Degradation of the network under low pH conditions was also demonstrated. Because these gels contain a tuneable proportion of amine groups and are based on Dexox, we believe that they have potential for future study in the context of injectable biomaterials for tissue engineering and drug delivery systems.

2. Materials and methods

2.1. Materials

N-Vinyl formamide (NVF, 98% purity), α,α′-azoisobutyronitrile (AIBN, 98%), poly(1-vinylpyrrolidone-co-vinyl acetate) (PVP-co-PVA, Mw ~50,000), ethanol (99%), sodium periodate (99.8%), N-Fmoc-1,3-propanediamine hydrobromide (96%, NFPD) 1, 8-diazabicyclo[5.4.0]undec-7-ene (DBU, 98% purity), dimethylformamide (DMF, 99.8% purity) and Dex (from *leuconostoc mesenteroides*) were supplied by Sigma (product no. 31,397) and used as received. Dex had an average molecular weight of about 60 kg/mol (supplier information). We selected the latter molecular weight, rather than Dex with a higher molecular weight, because 60 kg/mol Dex provided a good balance between ease of mixing of the pre-gelled mixtures (due to low viscosity) and good mechanical properties of the final composite (high modulus and yield strain). NVEE was synthesised and characterised using the methods described earlier [4]. Gold nanoparticles (Au NP) were citrate stabilised and supplied by Sigma–Aldrich with a size of 10 nm (supplier information). All water used was of high purity and was deionised prior to use.

2.2. PVAM microgel preparation

Following our previous approach [4], PVAM-BEVAME MGs were prepared by the hydrolysis of PNVF-NVEE particles. The synthesis for each dispersions is given below [30].

2.3. PNVF-NVEE microgel preparation

The following gives the preparation details for PNVF-9NVEE, which followed that reported earlier [4]. Briefly, the particles were prepared using non-aqueous dispersion polymerisation. NVF (6.0 g, 85.5 mmol), NVEE (1.8 g, 8.46 mmol) were added to a pre-purged 250 ml four-necked round bottomed flask containing EtOH (68 ml), PVP-*co*-PVA (1.8 g) and AIBN (0.241 g, 1.45 mmol). The temperature was maintained at 70 °C and polymerisation was conducted for 1 h under nitrogen. The product was purified by extensive washing/centrifugation and redispersion using EtOH.

2.4. PVAM-BEVAME microgel preparation

PVAM-BEVAME, which was the only microgel studied in this work and, for simplicity, is identified from this point onwards as MG. PNVF-NVEE particles (1.00 g) were isolated by centrifugation of the dispersion in 4 ml EtOH. The dispersion was added dropwise to 1 M NaOH (100 ml) which was stirred at 80 °C. The reaction was allowed to continue for 18 h. The MG particles were washed by centrifugation and redispersion in PBS (0.15 M) and then aqueous NaCl solution (0.15 M), which was followed by extensive washing with water.

2.5. Dextran oxidation

Dexox was prepared according to the method reported by Maia et al. [13] An aqueous solution of Dex (1.00 g; 12.5% (w/v)) was oxidised with aqueous sodium periodate solution (2 ml containing 2.46 mmol of $NaIO_4$) at room temperature for 4 h. The resulting Dexox was dialysed against water for 5 days. The theoretical extent of oxidation (% TO) for the Dex was calculated from the total number of Dex units that would have been oxidised if the reaction was 100% efficient. In this case the Dex was oxidised to 40% TO. In our hands, the *actual* degree of oxidation was calculated as 20.9% using an Fmoc loading assay (described below).

2.6. Fmoc loading assay

An Fmoc loading assay was used to measure the extent of Dex oxidation [41]. Dexox (12 mg) was dissolved in water (2 ml) and combined with an excess of NFPD (12.79 mg, 0.034 mmol). The theoretical aldehyde loading for this system was 4.93 mmol g^{-1}, based on the predicted TO of 40%. Unreacted mono-Fmoc diamine was removed by precipitation of the polymer in EtOH (10 ml), centrifugation (4 min, 7000 rpm) and decantation of the supernatant. The isolated polymeric product (Dexox-NFPD) was dried *in vacuo*. Dexox-NFPD (5.7 mg) was dissolved in DMF (10 ml) with DBU (0.2 g, 1.3 mmol) and the solution stirred at room temperature for 1 h. The solution was diluted to a polymer concentration of 0.0065 wt.% through addition of DMF. The absorption spectrum of this dilute solution was measured using a UV–visible spectrometer. In order to calculate the molar extinction coefficient (ε) of deprotected Fmoc groups in DMF/DBU, NFPD (26.02, 0.069 mmol) and DBU (0.4 g, 2.63 mmol) were dissolved in DMF (10 ml) and stirred for 1 h. The gradient of a linear plot of absorbance (A) at 305 nm vs. molar concentration (Fig. S1) was taken to be ε (L mol^{-1} cm^{-1}) multiplied by path length, l (cm). The actual value for the extent of oxidation of Dexox followed from quantification of the degree of the covalent reaction between NFPD and aldehyde groups of Dexox, using the following equation.

$$C_{ald} = \frac{[(A/\varepsilon l)V]}{m} \quad (1)$$

For the above equation, C_{ald}, V and m are the aldehyde loading (mol g^{-1}), solution volume (L) and the Dexox mass (g), respectively.

2.7. MG–Dexox composite preparation

MG–Dexox composite hydrogels consisted of Dexox and MG particle dispersion mixtures and were prepared at room temperature. The following example given is for MG–Dexox with a mass ratio (MR) of 2.0 and a MG particle concentration of 1.7 wt.%. Dexox solution (110 μl, 7.64 wt.%) was added dropwise at room temperature to a MG dispersion (140 μl, 3 wt.%) over a period of 30 s whilst the mixture was vortex mixed. The MR for the binary MG–Dexox mixtures is given by

$$MR = \frac{C_{Dexox}}{C_{MG}} \quad (2)$$

where C_{Dexox} and C_{MG} are, respectively, the MG and Dexox mass concentrations (wt.%). Control samples of Dex and MG particles (MG/Dex) were prepared in the same way as described above.

2.8. MG/Au nanoparticle mixture

Mixed MG/Au nanoparticle (NP) dispersions consisted of citrate stabilised Au nanoparticles added dropwise to MG particle dispersions. These mixed dispersions were prepared at room temperature. The concentrations used were calculated to give the same number of Au NPs as coils of Dexox in $MR = 0.7$ preparation. The Au NP solution (964 μl) was added dropwise at room temperature to a MG dispersion (36 μl, 0.37 wt.%) over a period of 30 s whilst the mixture was vortex mixed. The dispersion was allowed to equilibrate overnight before TEM samples were prepared.

2.9. Physical measurements

Photon correlation spectroscopy (PCS) measurements were performed using a BI-9000 Brookhaven light scattering apparatus (Brookhaven Instrument Cooperation), fitted with a 20 mW HeNe laser and the detector was set at a scattering angle of 90°. SEM measurements were obtained using a Philips FEGSEM instrument. Samples were dried at room temperature or by freeze-drying. For the turbidity studies, MG–Dexox mixtures were diluted to similar particle concentrations as those used for PCS (i.e., 0.05 wt.%) and the optical density (OD) was measured using UV–visible spectroscopy over the wavelength (λ) range 400–700 nm. The wavelength exponent (n-value) was obtained from the gradient of log(OD) versus log(λ) plots, i.e.,$=-d\log(\mathrm{OD})/d\log(\lambda)$. The magnitude of the n-value is very sensitive to aggregation and decreases significantly when aggregation occurs [9,42,43]. The morphology of MG and Au particles was investigated by TEM (Philips CM20 200 kV TEM). Dynamic rheology measurements were performed using a TA Instruments AR G2 temperature-controlled rheometer with an environmental chamber. A plate geometry (20 mm diameter) with a gap of 250 μm was used for the rheology experiments. For the strain-amplitude measurements a frequency of 1 Hz was used. A strain of 0.1% was used for the frequency-sweep measurements. The MG particle concentration was fixed at 1.7 wt.% for all rheology experiments considered in this study.

3. Results and discussion

3.1. Characterisation of the partially oxidised dextran

The Dex used for this study had a molecular weight of 60,000 g/mol, and the actual extent of oxidation for Dexox was calculated as 20.9% using the Fmoc loading assay (see Section 2). Each Dexox chain has an average of approximately 77 oxidised repeat units. Oxidised Dex residues each have two aldehyde groups, which were available to react with primary amines from the MG particles in the crosslinking reaction (Scheme 1). The hydrodynamic radius of the Dex has been reported in the literature for a range of molecular weights and we have taken this as 5.4 nm [44]; a value which is two-to-three orders of magnitude smaller than the hydrodynamic diameter of the MG particles (below).

3.2. Characterisation of the PVAM microgel particles

Fig. 1(a) and (b) shows SEM and optical images, respectively, of the MG particles. The SEM image shows collapsed MG particles with an approximate size of 350 nm, which is comparable to the size reported earlier [4]. Fig. 1(b) shows a representative optical image of the MG particles dispersed in water at pH = 9.3. Here, the MG particles were in their swollen state and the hydrodynamic radius was 800 nm. The zeta potential (ζ) was measured as +20.4 mV for the particles at pH 9.3, which is a value that is consistent with their high primary amine group content. The conversion of PNVF MG to PVAM MG was considered successful based on these properties as well as FTIR data (see Fig. S2). For example the spectrum for PVAM MG (Fig. S2) is identical to that reported earlier for PVAM MGs [4]. The characteristic amide I and II bands (at 1650 and 1540 cm^{-1} respectively) were not evident in the spectrum for PVAM-BEVAME MG and a new RNH_2 peak at 1590 cm^{-1} was present [45]. All work considered from this point onwards involved only PVAM MG particles.

3.3. Effect of added oxidised dextran on dilute microgel dispersions

To examine whether an attractive interaction occurred between MG and Dexox we initially investigated dilute mixed dispersions. Here *MR* was varied using samples whilst the MG particle concentration was fixed at 0.05 wt.% The effects of the MG–Dexox reaction could be seen visually from the samples shown in the upper row of Fig. 2. The mixtures of MG and Dexox became increasingly turbid at higher *MR* values. The *MR* = 5 mixture was the most visually turbid and some aggregates were visible. By contrast, for the control MG/Dex mixtures (lower row of Fig. 2) the turbidity remained constant and was not affected by added Dex. This observation indicates a specific attractive interaction occurred between PVAM and Dexox. The aggregation is attributed to the MG particles adhering to one another via Dexox bridging aggregation mediated, in turn, by reaction of aldehyde with primary amine groups.

OD values measured at 400 nm (OD400) and n-values for dilute MG–Dexox and MG/Dex dispersions were measured (see Fig. 3(a) and (b)) to more closely study the extent of Dexox-triggered aggregation of the MG particles. There was a small initial increase of OD400 for the MG/Dex mixtures. By contrast, OD400 increased strongly for the MG–Dexox systems when *MR* reached 2.0, where the aggregation was strong enough to affect OD400. Fig. 3(b) gives the variation of the magnitude of the n-values with *MR* for the same dispersions. For MG–Dexox dispersions, the n-value magnitude decreased for *MR* greater than or equal to 0.7. As the n-value is very sensitive to aggregation [43], the critical *MR* value (MR_{CRIT}) for the aggregation is taken as $MR_{CRIT} = 0.7$ for MG–Dexox. This value corresponds to sufficient Dexox linkages between MG particles to cause particle aggregates to form. By contrast there was no effect from MR on the n-value data for the control MG/Dex dispersions. This result indicates that Dex was not able to form covalent linkages with the MG particles, which is due to an absence of aldehyde groups for this non-oxidised polymer.

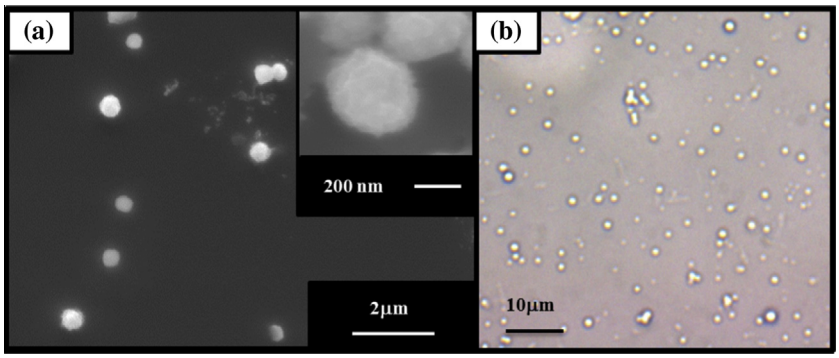

Fig. 1. PVAM MG particle characterisation. (a) SEM image and (b) optical image of the PVAM MG particles. For (b) the particles were dispersed at a pH of 9.3.

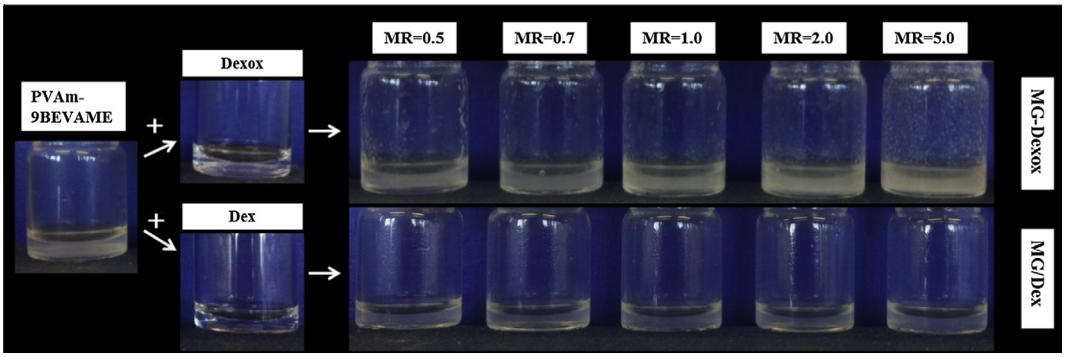

Fig. 2. Aggregation of mixed MG–Dexox dispersions. The images show digital photographs of dilute mixed dispersions of MG particles and Dexox with varying *MR* values (shown above tubes).

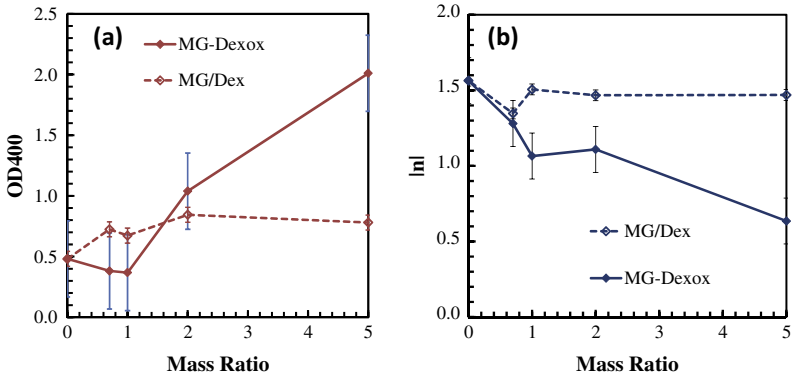

Fig. 3. Colloidal stability data for dilute MG–Dexox and MG/Dex dispersions with varied mass ratio. (a) Shows the variation of OD400 with *MR* and (b) shows the variation of the *n*-value with *MR*. The lines are guides to the eye.

3.4. Morphology and mechanical properties of composite microgel–oxidised dextran gels

We investigated concentrated dispersions of MG particles and Dexox to study gel formation. All of the concentrated dispersions studied here contained a MG concentration of 1.7 wt.%. A digital photograph of concentrated mixed MG–Dexox and MG/Dex dispersions is shown in Fig. 4. The MG/Dex sample (upper right) flowed; whereas, the MG–Dexox sample (lower left) stayed in place and was a gel. Gel formation occurred rapidly (over a period of seconds) upon mixing of the MG dispersion and Dexox solution.

The morphologies of the mixed gels were investigated using SEM. Fig. 5(a) shows a representative image for the pure freeze-dried MG particles. For comparison, an SEM image of the ribbon/sheet-like Dexox sample is shown in Fig. 5(b). The other images shown are for MG–Dexox mixtures at *MR* = 2.0 (Fig. 5(c)) and 5.0 (Fig. 5(d)). For the *MR* = 2.0 mixed gel (Fig. 5(c)) the particles were tightly aggregated. For the SEM image of MG–Dexox with *MR* = 5.0 there are smooth areas (highlighted) that are due to excess Dexox. There was a general lack of close packing and voids were present for the MG–Dexox gels, as probed by SEM, which indicates that a space-filling morphology occurred for these gels. This is typical of the morphology expected for aggregated particles.

The mechanical properties of the MG–Dexox gels formed from concentrated dispersions were investigated using dynamic rheology. Frequency-sweep data for MG–Dexox obtained using a range of *MR* values are shown in Fig. 6(a) and (b). (For comparison, frequency-sweep data for the control MG/Dex systems in Fig. S3.) The data shown in Fig. 6(a) and (b) generally show low frequency dependences for both G' (storage modulus) and G'' (loss modulus). The fact that the G' values were much greater than G'' indicates that

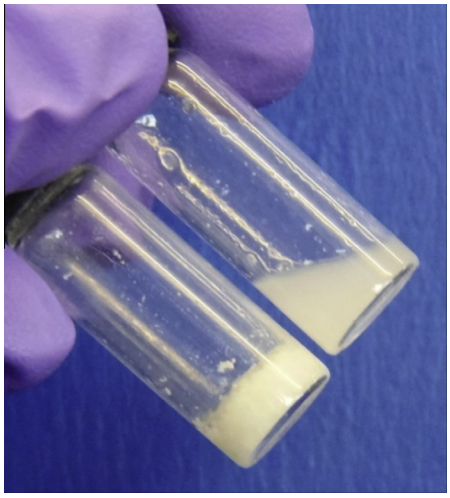

Fig. 4. Digital photographs of concentrated MG–Dexox (lower left) and MG/Dex (upper right) dispersions. The *MR* value was 2.0.

gels had been formed. The data shown for *MR* = 0 in Fig. 6(a) correspond to the pure MG, i.e., a soft physical homoparticle gel of MG particles. As Dexox was added (and *MR* increased) the G' and G'' values increased and their frequency dependence decreased. This indicates the added Dexox chains provided elastically effective linkages which enhanced the distribution of stress within the network. By contrast the G' and G'' values for the MG/Dex physical gels remained low (Fig. S3) and were not greatly affected by added Dex. These differences in rheology further support our proposal that the MG–Dexox gels comprised covalent networks (Scheme 1).

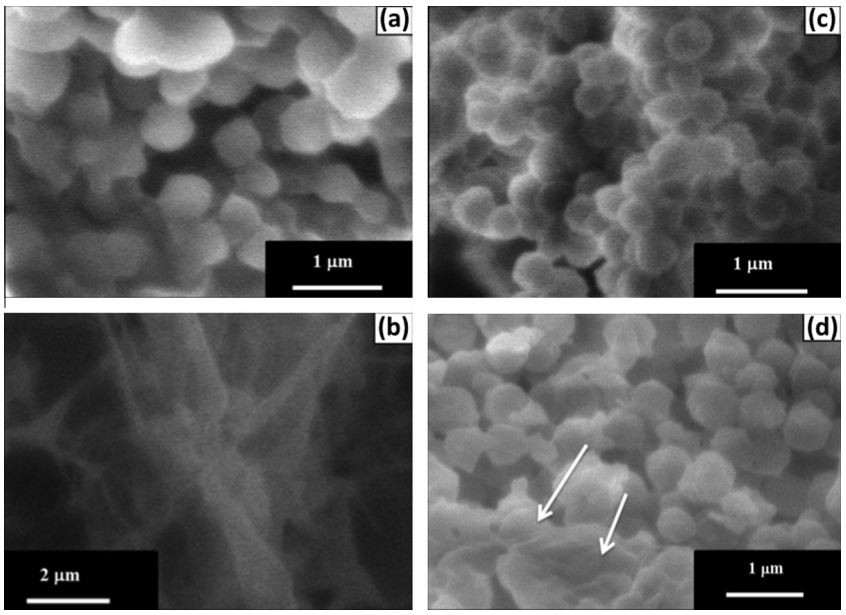

Fig. 5. Morphologies of gels and dispersions. Freeze-dried SEM images are shown. The *MR* values were (a) 0 (MG particles only), (b) Dexox only (1.7 wt.%) (c) MG–Dexox with *MR* = 2.0 and (d) MG–Dexox with *MR* = 5.0. The arrows in (d) highlight the smooth areas between MG particles which are proposed to be due to Dexox.

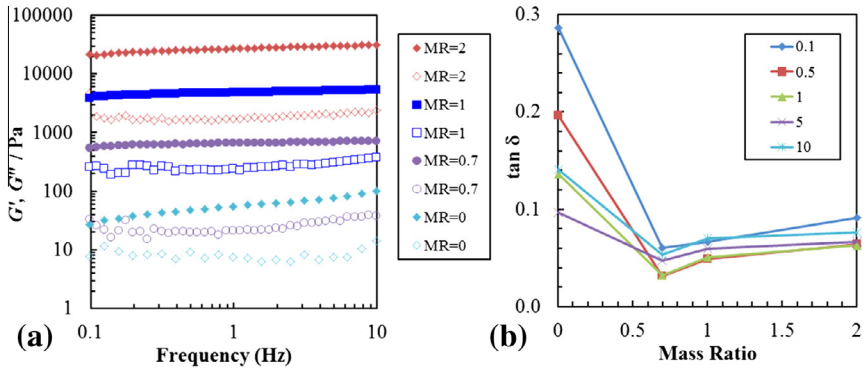

Fig. 6. Frequency-sweep data for MG–Dexox gels. (a) shows G' (closed symbols) and G'' (open symbols) as a function of frequency. (b) Shows the variation of $\tan\delta$ with *MR* for selected frequencies (Hz, legend).

Fig. 6(b) shows $\tan\delta$ values (= G''/G') measured at selected frequencies plotted as a function of *MR*. Similar plots for other gels have been used to establish gelation points [46]. The frequency dependency for $\tan\delta$ is well known to reach zero at the gel point [47]. Although the $\tan\delta$ values do not completely overlap, it is clear from Fig. 6(b) that their spread is narrower once *MR* reaches 0.7. We conclude from these data that the network approached the ideal gel point at MR_{CRIT}, which was identified from the turbidity studies above.

We probed the ductility of the gels using strain-sweep measurements. Data for MG–Dexox are shown in Fig. 7(a) and (b). The data show that G' was constant at low strain values, before an increase occurred (strain hardening) for *all* systems. This increase was followed by a subsequent decreases for G' and G''. The G' data passed through the maxima for G'' which implies strain-induced network breakdown coincided with maximum energy loss (dissipation). The appearance of a single maximum for G'' (and one-step yielding) has been attributed to cage breaking for colloidal glasses comprised of soft MG particles [48]. Because this maximum is present for the G'' data from the pure MG precursor it follows that a similar structural breakdown applies for the MG–Dexox gels. Presumably, Dexox reinforced these structures by providing inter-MG particle linkages. The data for MG–Dexox contrast to those for the MG/Dex physical gels (Fig. S4) where the addition of Dex failed to significantly increase the G' and G'' values.

Fig. 8(a) shows the G' values of the MG–Dexox and MG/Dex gels as a function of *MR*. The G' values for MG–Dexox system increased exponentially with *MR*. Thus, the networks became better able to store energy effectively with increasing Dexox. Even a small amount of Dexox, such as $MR = MR_{CRIT} = 0.7$, could increase G' by a factor of ca. 2.0 compared to the pure MG gel. The increase of G' reached a plateau at *MR* = 2.0. This trend suggests that an optimum *MR* for network connectivity and stress distribution was achieved at *MR* = 2.0. By contrast, for the control MG/Dex gels the presence of Dex decreased the G' values. This result is due to the inability of Dex to form covalent linkages with the MG network. The difference of G' at *MR* = 2.0 for the two gels (Fig. 8(a)) is striking. *Replacement of Dex with Dexox caused a G' increase by ~ 5 orders of magnitude.*

The ductility of the gels was assessed through the yield strain (γ^*), which corresponds to the strain (γ) values at which $\tan\delta = 1$. The relationship between γ^* and *MR* for both systems is shown in Fig. 8(b). For the MG–Dexox system, the γ^* values increased

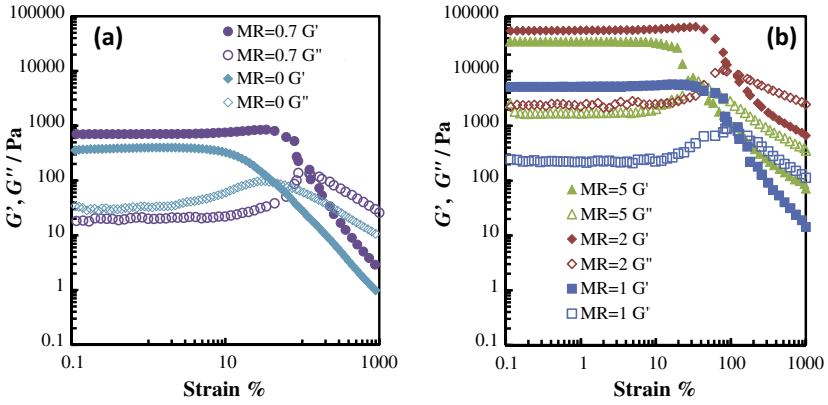

Fig. 7. Strain-sweep rheology data for MG–Dexox gels. The *MR* values are shown in the legends. Values for G' and G'' are shown as closed and open symbols, respectively.

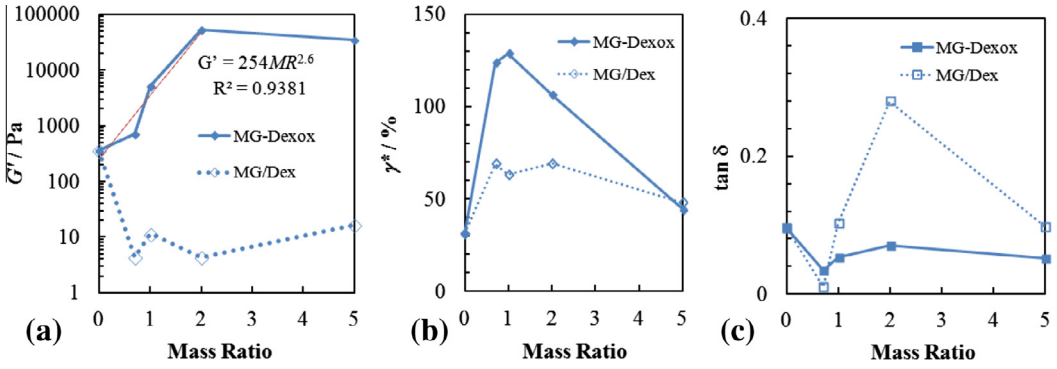

Fig. 8. Effect of mass ratio on composite gel mechanical properties. Variation of G' (a), yield strain (b) and $\tan\delta$ (c) with *MR* for concentrated MG–Dexox and MG/Dex dispersions. The red line in (a) is a line of best fit for the first four data points (equation for fit is shown). The other lines are guides for the eye. (For interpretation of the references to colour in this figure legend, the reader is referred to the web version of this article.)

strongly with *MR* between *MR* values of 0 and 0.7. Although the maximum γ^* is at *MR* = 1.0, the γ^* remained comparable between *MR* = 0.7 and 2.0, after which it decreased. Above *MR* = 2.0 the added Dexox decreased the ductility. The same general trends were apparent for the control MG/Dex samples, implying that the enhancements of γ^* were accentuated by formation of covalent linkages between Dexox and the MG particles. Clearly, the increase of the ductility for these gels was due to Dexox; however, the effect was optimised in terms of modulus and ductility by the combination of MG particles and Dexox.

The data shown for MG–Dexox in Fig. 8(a) and (b) are remarkable in that G' increases with *MR* and γ^* also remained high. Normally, modulus and yield at break are inversely related. Our data indicate that the two physical processes responsible for modulus and maximum chain stretching were decoupled for these new gels. Moreover, the MG–Dexox gel with *MR* = 2.0 was exemplary because it had a G' of 54 kPa and a γ^* value of 125% for a gel containing a total polymer concentration of only ca. 5 wt.%. This modulus value is far higher than modulus values reported for composite gels consisting of microgel particles embedded in hydrogels [38,39].

The variation of $\tan\delta$ is shown in Fig. 8(c) for MG–Dexox and MG/Dex as a function of *MR*. In most cases the $\tan\delta$ is lower for MG–Dexox compared to MG/Dex. The $\tan\delta$ data show a minimum for MG–Dexox at *MR* = 0.7, which is the MR_{CRIT} value identified from the data shown in Fig. 6(b)). Moreover, these data clearly show the increased $\tan\delta$ values for the MG/Dex systems at the mid-range *MR* values, which implies a higher proportion of the total energy was dissipated as a result of strain for those non-covalently inter-linked physical gels.

An interesting question concerns the value for *MR* at which the MG particles could be expected to be fully covered by Dexox polymer chains. The latter value ($MR^{\#}$) can be estimated using a close-packed Dexox monolayer around all of the MG particles. For $MR > MR^{\#}$, no crosslinks should be formed between neighbouring MG particles because every amine site for each MG particle would be connected to an aldehyde via the surface adsorbed Dexox. It is easy to show from a simple geometric model in which Dexox spheres (5.4 nm) covered spherical MG particles (800 nm) that the $MR^{\#}$ for the MG–Dexox system is 0.012. However, MR_{CRIT} (=0.7) $\gg MR^{\#}$. Possible reasons for this unexpected behaviour are that gel formation was depletion flocculation assisted, which required a relatively high concentration of non-adsorbing polymer [49]. Additionally, relatively few binding sites may have been present because the Dexox chains had an experimentally determined degree of oxidation of 20.9% and more chains would have been required to link with available primary amine sites. A third explanation for $MR_{CRIT} \gg MR^{\#}$ is penetration of the exterior of the MG particles by Dexox chains. Penetration of the peripheries of MG particles by macromolecules has been reported elsewhere [50]. The first two explanations considered above appear reasonable and are likely to have contributed to the relatively high MR_{CRIT} value. The last explanation is discussed further below.

3.5. Mixed microgel/gold nanoparticle dispersions

To determine if the Dexox and Dex could penetrate the MG particle peripheries the MG pore size was qualitatively investigated by mixing the MG particles with 10 nm gold nanoparticles (Au NP) and examining them using TEM. We sought to establish whether

Au NPs could penetrate the MG particles. The Au NPs were negatively charged ($\zeta = -33$ mV), due to citrate stabilisation [51]. On the other hand the MG particles were positively charged (above). Fig. 9 shows TEM images obtained for MG/Au NP mixtures, MG particles and also individual NP particles. The Au NPs were visible at the MG particle periphery as can be seen from Fig. 9(a) and the inset. It follows from the TEM data that the Au NPs were *not* able to penetrate the MG particles. In the absence of significant triggered collapse of the MG particle periphery caused by the negatively charged Au NPs, these data would indicate a pore size less than 10 nm. However, triggered collapsed has been reported for related studies involving microgel particles and oppositely charged peptides [52] and this type of complication cannot be ruled out for the present study. Because oppositely charged units can enter the interior of oppositely charged microgels [50], it is not clear whether collapse of the periphery in the vicinity of the Au NPs would prevent their migration to the interior if the pores were much larger than the diameter of the Au NPs. We propose that our data are consistent with the absence of pores that are very large compared to the Au NP size.

From the discussion above it can be further proposed that penetration of the periphery of the MG particles by Dexox (which should have been uncharged) did not contribute to the high *MR* values required to trigger aggregation and network formation, i.e., $MR_{CRIT} \gg MR^{\#}$. Accordingly, the inefficient binding of Dexox to the primary amine groups was the primary cause for the relatively high *MR* values observed in this study. We note that the present TEM image shown in Fig. 9(a) is consistent with a surface that is rich in primary amine groups and is the first example reported of Au NPs decorating PVAM MGs.

3.6. pH-Triggered degradation of MG–Dexox gels

Imine bonds are well known to cleave at low pH (below pH 6.8) [18,53]. In order to examine whether disassembly of the network could occur for our MG–Dexox gels, rheology was used to measure pH-dependence of G'. Rheological studies were conducted on the original MG–Dexox sample prepared as described above ($MR = 2.0$). To this gel concentrated HCl solution or the same volume of water (a control) was carefully added with mixing. The MG particle concentration after dilution was 1.5 wt.%. Dynamic rheology experiments were conducted before and 16 h after the additions (Fig. 10). The pH values after HCl addition or water were 3.3 and 9.0, respectively. (A pH of 3.3 is much lower than that required for the cleavage reaction and was selected to accelerate gel breakdown.) The G' and G'' data for the systems are shown as a function of frequency (Fig. 10(a)) and as a function of strain (Fig. 10(b)). The G' for the original sample was 30,850 Pa; whereas, when water was introduced the G' decreased to 19,700 Pa which is lower due to dilution and mixing. Interestingly, when the pH of the system was lowered to 3.3 by HCl addition the G' value dramatically decreased to 2100 Pa (i.e., only 10% of the original value for the sample). The γ^{*} also decreased from ~180% strain with added water to 30% (Fig. 10(b)) due to HCl addition. Moreover, the frequency dependent G'' data (Fig. 10(a)) shows a minimum, which indicates greater MG particle motion during the strain fluctuations. These major decreases in mechanical performance for the MG–Dexox gels upon addition of HCl are strong evidence for cleavage of crosslinks (imine groups) and disruption of the elastic networks which previously allowed energy to be stored within the gels. The acid-triggered gel disassembly process was not 100% efficient over the

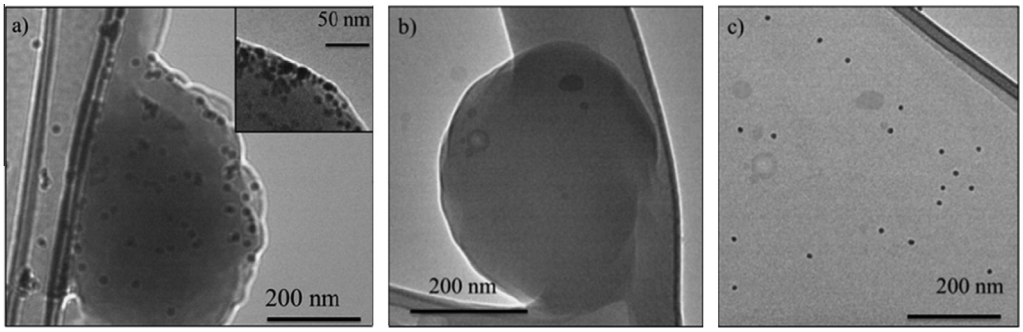

Fig. 9. Testing for evidence of nanoparticle penetration of the microgel particles. TEM image of (a) MG particles combined with Au nanoparticles, (b) MG particle only and (c) Au NPs only.

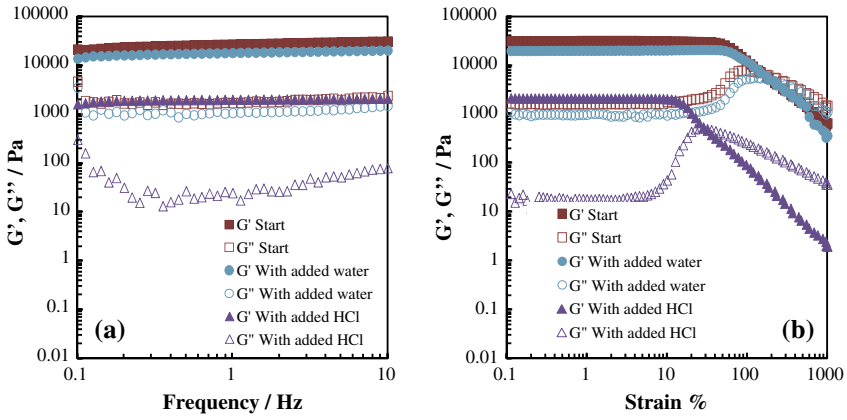

Fig. 10. Acid-triggered gel degradation for MG–Dexox gels. (a) Shows frequency-sweep data and (b) shows strain-sweep data. The data are shown for the gels before or after HCl or water of the same volume. See text. Values for G' and G'' are shown as closed and open symbols, respectively.

time limited period studied here because the G' for the HCl-treated sample was still relatively high compared to that for an equivalent MG/Dex sample (e.g., $MR = 2.0$ in Fig. S4(b)).

The data discussed above were explained in terms of acid-triggered imine cleavage (Scheme 1). A referee pointed out that another possibility is that aminal structures formed. An example of aminal formation is known for PVAM reactions (Scheme 14 of Ref. [24]). The latter groups could conceivably provide more robust crosslinks. Given that pH-triggered gel breakdown occurred for our gels the data favour our assumption of imine formation. However, we cannot rule out the presence of a minor proportion of aminal crosslinks.

3.7. Proposed mechanism for MG–Dexox gel formation

The gel formation demonstrated by rheological data discussed above shows that the Dexox contributed elastically effective chains between the MG particles. However, the *MR* values required to provide evidence of aggregation (for dilute dispersions) and G' increases (for concentrated dispersions) were much higher than $MR^{\#}$. In addition, evidence for highly permeable MG peripheries was *not* found using Au NPs. Whilst the Dexox chains were probably smaller than the Au nanoparticles, there is no evidence that penetration occurred. Accordingly, it is suggested that inefficient crosslinking between amine groups and aldehyde groups was responsible for the relatively high MR_{CRIT} values in this study. Fig 11 illustrates the structures we propose for MG–Dexox gels. At low *MR* values, e.g. $MR = 0.7$, Dexox did not fully cover the surface and sparse cross-links were formed between the MG particles. This proposal was supported by the relatively modest difference of G' for $MR = 0$ and $MR = 0.7$. At $MR = 2.0$ the Dexox covered most of the particles and gave enough cross-links to form an effective elastic network in which neighbouring particles were covalently interconnected. Once *MR* reached 5.0, Dexox may have covered more of the MG particles than required for optimum network connectivity and the ductility of the gels decreased. $MR = 2.0$ corresponded to the optimum conditions for formation of gels with high modulus and ductility.

The increase of *both* G' and γ^* at the lower *MR* values (Fig. 8(a) and (b)) requires additional comment. Nanocomposite gels are well known to exhibit both high modulus and ductility, as a consequence of the laponite sheets acting as crosslinking points [54]. In the present case the MG particles can be viewed as macro-crosslinking units. Increasing the *MR* value may increase the number-density of elastically effective chains whilst maintaining (or even increasing) the separation between the crosslinking units (MG particles). The former effect would increase the modulus and the latter could maintain (or increase) the yield strain.

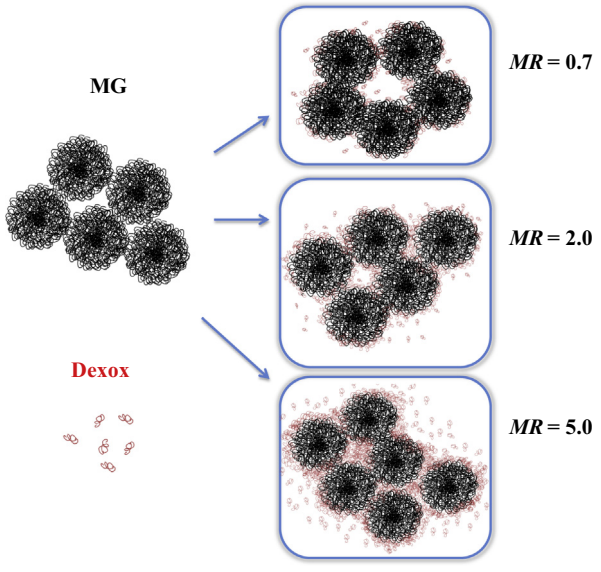

Fig. 11. Diagram of proposed mechanism for MG–Dexox gel formation.

4. Conclusions

We have investigated a novel family of hydrogel composites composed of stimuli responsive MG particles and added Dexox. The reaction between the aldehyde groups in Dexox and primary amine groups in the MG particles resulted in cross-links forming between the two components. These linkages formed an elastic network containing the MG particles and resulted in gel formation with good mechanical properties. The inclusion of the Dexox chains resulted in high ductility gels as compared with gels prepared without added Dexox. These new gels achieved an increase in both the stiffness and ductility for most of the *MR* values studied. This result is unexpected, but potentially has useful applications. We took advantage of the imine groups to demonstrate considerable pH-triggered disassembly of the network. Reversible assembly of gels has many potential uses, for example in targeted drug delivery. We have also demonstrated that Au nanoparticles adsorbed onto the surface of the MG particles, which is a new observation for these MGs. The attractive interaction between Au nanoparticles and the MG could have wider implications in the context of MG/metal nanoparticle composite preparation as well as other aldehyde-containing polymers.

Acknowledgments

BRS would like to thank the EPSRC for funding this research.

Appendix A. Supplementary material

Supplementary data associated with this article can be found, in the online version, at http://dx.doi.org/10.1016/j.jcis.2014.09.041.

References

[1] Z. Wang, R. Pelton, Langmuir 30 (2014) 6763–6767.
[2] C.H. Hofmann, F.A. Plamper, C. Scherzinger, S. Hietala, W. Richtering, Macromolecules 46 (2012) 523–532.
[3] B.H. Tan, K.C. Tam, D. Dupin, S.P. Armes, Langmuir 26 (2009) 2736–2744.
[4] S. Thaiboonrod, C. Berkland, A.H. Milani, R. Ulijn, B.R. Saunders, Soft Matter 9 (2013) 3920–3930.
[5] V.M. Chauhan, G.R. Burnett, J.W. Aylott, Analyst 136 (2011) 1799–1801.
[6] C.A. Prestidge, T.J. Barnes, C.-H. Lau, C. Barnett, A. Loni, et al., Expert Opin. Drug Delivery 4 (2007) 101–110.
[7] B.R. Saunders, B. Vincent, Adv. Colloid Interface Sci. 80 (1999) 1–25.
[8] W. Richtering, B.R. Saunders, Soft Matter 10 (2014) 3695–3702.
[9] S. Tungchaiwattana, R. Liu, S. Halacheva, N.N. Shahidan, A. Kells, et al., Soft Matter 9 (2013) 3547.
[10] J. Hu, K. Hiwatashi, T. Kurokawa, S.M. Liang, Z.L. Wu, et al., Macromolecules 44 (2011) 7775–7781.
[11] D. Suzuki, K. Horigome, Langmuir 27 (2011) 12368–12374.
[12] J.K. Armstrong, R.B. Wenby, H.J. Meiselman, T.C. Fisher, Biophys. J. 87 (2004) 4259–4270.
[13] J. Maia, L. Ferreira, Polymer 46 (2005) 9604–9614.
[14] J. Maia, M. Ribeiro, Acta Biomater. 5 (2009) 1948–1955.
[15] D. Sivakumaran, D. Maitland, Macromolecules 12 (2011) 4112–4120.
[16] K.H. Bouhadira, D.S. Hausman, D.J. Mooney, Polymer 40 (1999) 3575–3584.
[17] J. Maia, R. Carvalho, Polymer 52 (2011) 258–265.
[18] X. Xu, J.D. Flores, C.L. McCormick, Macromolecules 44 (2011) 1327–1334.
[19] Y. Qiu, T. Zhang, M. Ruegsegger, R.E. Marchant, Macromolecules 31 (1998) 165–171.
[20] S. Thaiboonrod, A.H. Milani, B.R. Saunders, J. Mater. Chem. B 2 (2014) 110.
[21] R. Widenbring, G. Frenning, M. Malmsten, Biomacromolecules (2014), http://dx.doi.org/10.1021/bm5009525.
[22] J. Shin, P. Shum, D.H. Thompson, J. Controlled Release 91 (2003) 187–200.
[23] J.P. Karam, C. Muscari, C.N. Montero-Menei, Biomaterials 33 (2012) 5683–5695.

[24] R.K. Pinschmidt, J. Polym. Sci. Polym. Chem. 48 (2010) 2257.
[25] R.K. Pinschmidt, W.L. Renz, W.E. Carroll, K. Yacoub, J. Drescher, et al., J. Macromol. Sci. Pure 34 (1997) 1885–1905.
[26] S. Khondee, T. Yakovleva, C. Berkland, J. Appl. Polym. Sci. 118 (2010) 1921–1932.
[27] J. McCann, S. Thaiboonrod, R.V. Ulijn, B.R. Saunders, J. Colloid Interface Sci. 415 (2014) 151–158.
[28] J. Xu, A. Barros Timmons, R. Pelton, Colloid Polym. Sci. 282 (2004) 256–263.
[29] C. Miao, X. Chen, R. Pelton, Ind. Eng. Chem. Res. 46 (2007) 6486–6493.
[30] S. Thaiboonrod, C. Berkland, A.H. Milani, R.V. Ulijn, B.R. Saunders, Soft Matter 9 (2013) 3920.
[31] Z. Mohammadi, A. Cole, C. Berkland, J. Phys. Chem. C 113 (2009) 762–768.
[32] C. Chen, M. Liu, S. Lu, C. Gao, J. Chen, J. Biomater. Sci. Polym. Ed. (2011).
[33] J. Zhang, X.-D. Xu, Y. Liu, C.-W. Liu, X.-H. Chen, et al., Adv. Funct. Mater. 22 (2012) 1704–1710.
[34] L. Wang, X. Wang, Langmuir 24 (2008) 1902–1909.
[35] L. Wang, J. Sun, J. Mater. Chem. 18 (2008) 4042–4049.
[36] X. Jia, Y. Yeo, R.J. Clifton, T. Jiao, D.S. Kohane, et al., Biomacromol 7 (2006) 3336–3344.
[37] N. Huang, Y. Guan, X.X. Zhu, Y. Zhang, ChemPhysChem 15 (2014) 1785–1792.
[38] J. Meid, F. Dierkes, J. Cui, R. Messing, A.J. Crosby, et al., Soft Matter 8 (2012) 4254–4263.
[39] D. Sivakumaran, D. Maitland, T. Oszustowicz, T. Hoare, J. Colloid Interface Sci. 392 (2013) 422–430.
[40] W. Song, Y. Guan, Y. Zhang, X.X. Zhu, Soft Matter 9 (2013) 2629–2636.
[41] M. Gude, J. Ryf, P.D. White, Lett. Pept. Sci. 9 (2002) 203–206.
[42] O. Pinprayoon, R. Groves, B.R. Saunders, J. Colloid Interface Sci. 321 (2008) 315–322.
[43] J.A. Long, D.W.J. Osmond, J.B. Vincent, J. Colloid Interface Sci. 42 (1973) 545.
[44] E. Antoniou, M. Tsianou, J. Appl. Polym. Sci. 125 (2012) 1681–1692.
[45] L. Shi, C. Berkland, Macromolecules 40 (2007) 4635–4643.
[46] S.A. Madbouly, J.U. Otaigbe, Macromolecules 38 (2005) 10178–10184.
[47] H.H. Winter, J. Rheol. 30 (1986) 367.
[48] Z. Zhou, J.V. Hollingsworth, S. Hong, H. Cheng, C.C. Han, Langmuir 30 (2014) 5739–5746.
[49] P. Jenkins, M. Snowden, Adv. Colloid Interface 68 (1996) 57–96.
[50] J. Kleinen, A. Klee, W. Richtering, Langmuir 26 (2010) 11258–11265.
[51] R. Prado-Gotor, G. Lopez-Perez, M.J. Martin, F. Cabrera-Escribano, A. Franconetti, J. Inorg. Biochem. 135 (2014) 77–85.
[52] H. Bysell, M. Malmsten, Langmuir 25 (2008) 522–528.
[53] G.A. Lemieux, C.R. Bertozzi, Trends Biotechnol. 16 (1998) 506–513.
[54] K. Haraguchi, T. Takehisa, Adv. Mater. 14 (2002) 1120–1124.